Indian Journal of Chemistry
Vol. 41A, April 2002, pp. 692-700

Effect of vanadia on physico-chemical and catalytic characteristics of dysprosia

S Sugunan* & N K Renuka

Department of Applied Chemistry, Cochin University of Science and Technology, Kochi 682 022, India

Received 7 June 2001; revised 27 December 2001

Physico-chemical characterization of Dy_2O_3/V_2O_5 systems prepared through wet impregnation method has been carried out using various techniques like EDX, XRD, FTIR, thermal studies, BET surface area, pore volume and pore size distribution analysis. The amount of vanadia incorporated has been found to influence the surface properties of dysprosia. The spectroscopic results combining with X-ray analysis reveal that vanadia species exist predominantly as isolated amorphous vanadyl units along with crystalline dysprosium orthovanadate. Basicity studies have been conducted by adsorption of electron acceptors and acidity and acid strength distribution by temperature programmed desorption of ammonia. Cyclohexanol decomposition has been employed as a chemical probe reaction to examine the effect of vanadia on the acid base property of Dy_2O_3. Incorporation of vanadia titrates the Lewis acid and base sites of Dy_2O_3, while an enhancement of Bronsted acid sites has been noticed. Data have been correlated with the catalytic activity of these oxides towards the vapour phase methylation of phenol.

The major advantage of multicomponent metal oxide catalytic systems is that it is possible to tune oxygen sorption properties and acid base properties by meticulously choosing the required metal oxide components. In this line, supporting an active metal oxide over another oxide with required physical and chemical properties has opened an innovative way to resourceful catalysts. The fine dispersion of the active species on the support makes supported system dominate over bulk oxides. Support reduces sintering of the active metal oxide and hence induces an enhancement in the effective surface area and also serves as a heat conduction medium. Apart from this, supports are used to improve mechanical strength, thermal stability and lifetime of the active metal species.

Among these supported systems, vanadia based catalysts are renowned for their activity towards various types of partial or selective oxidation reactions, where pure vanadia leads to undesirable complete oxidation products. Considerable research has been focussed on this class of catalysts to obtain an idea of the nature and reactivity of supported vanadia catalysts which was found to be well pertinent for industrially significant reactions like oxidation, ammoxidation, selective catalytic reduction etc.[1-4]. Support - vanadia interaction, which results in the stabilization, can be viewed either in terms of minimization of surface free energy or in terms of formation of new chemical compounds. The actual structure of vanadia species present in the system will depend amongst other things on the chemical nature and crystal structure of the support, the vanadium loading, and on the presence of adventitious impurities. Structure and physico-chemical properties of supported metal oxides are different when compared with bulk metal oxides, because of their interaction with supports[5]. Preferential formation of compounds occurs on basic supports due to the strong interaction between comparatively acidic vanadia and the support. On acidic supports, vanadia species have negligible interaction with the support, which aggregate to form V_2O_5 crystallites. Accordingly, V_2O_5 crystals are observed on silica[6]; vanadates are formed on magnesium oxide[7].

Present study intends to analyse the effect of vanadia on dysprosia prepared through wet impregnation (excess solvent) method. Only a few reports (mainly confined to activity towards oxidative dehydrogenation reactions) are available in the literature using rare earth oxide supports[8]. Dysprosia being a basic oxide, Dy/V systems are expected to be good oxidative dehydrogenation catalysts. Nature of interaction of the two oxides is followed using different characterization techniques and the influence of vanadia on the physico-chemical characteristics is analysed in detail. Catalytic activity of Dy/V system is tested for the alkylation of phenol with methanol. The effect of acid base property of the catalyst on the activity and selectivity towards methylation of phenol has already been reported[9-12].

Materials and Methods

Catalyst synthesis

Pure dysprosia was prepared by the hydrolysis of nitrate salt using aqueous ammonia. The precipitate was filtered, washed and dried overnight at 110°C and was calcined at 400°C to get the oxide. Supported systems were prepared by adopting wet impregnation method by stirring the support with an oxalic acid solution of ammonium metavanadate[13]. Different compositions of vanadia were selected, namely, 3, 7, 11 and 15 wt%. They were named according to their vanadia % as D3, D7, D11 and D15. Pure Dy_2O_3 is denoted as D.

Physico-chemical characterisation

The chemical composition of the supported system was determined by energy dispersive analysis (Stereoscan 440 Cambridge, UK). The crystallinity of the samples was determined by the powder XRD method by a Rigaku D-max C X-ray diffractometer using Ni filtered Cu-Kα adiation (λ = 1.5406Å). The FTIR spectra were recorded using a Shimadzu spectrophotometer (DR 8001) in the range 400-4000 cm^{-1}. Surface area of the catalysts were measured using a Micromeritics Gemini Surface area analyser by low temperature nitrogen adsorption method. Pore volume and pore size distribution were determined by Quantachrome Autoscan –92 porosimery, USA. Shimadzu thermogravimetric analyser (TGA-50) was used to determine the thermal stability of the supported systems.

The evaluation of surface acidity was carried out by vapour phase decomposition of cyclohexanol and temperature programmed desorption (TPD) of ammonia. The alcohol decomposition reaction was performed in gas phase and the products were analysed by GC fitted with a 6′×1/8″ stainless steel column packed with 5% NPQSB + H_3PO_4 on anachrom A 80/100 mesh. For TPD studies, pelletised catalyst was activated inside the reactor under nitrogen flow for half an hour. After cooling to room temperature, ammonia was injected in the absence of the carrier gas flow and the system was allowed to attain equilibrium. The excess and physisorbed ammonia was flushed out by a current of nitrogen. The temperature was then raised in a stepwise manner at a linear heating rate of about 20°C/min. The ammonia desorbed at temperature ranges of 100°C was trapped in dilute sulphuric acid solution and estimated volumetrically by back titration with NaOH.

Electron donor property study using electron acceptors was performed to get an insight to Lewis basicity of the catalysts. The experimental procedure involves stirring a weighed amount of the catalyst with different concentrations of electron acceptors (EA) in acetonitrile solvent. The amount of EA adsorbed was determined by measuring the absorbance of the solution at the λ_{max} of the EA using a UV-VIS spectrophotometer (Shimadzu UV- 160 A) before and after adsorption. The limiting amount adsorbed was obtained from Langmuir plots. The electron acceptors selected for the study were tetracyanoquinodimethane (TCNQ), chloranil and *p*-dinitrobenzene (PDNB); their electron affinity being 2.84, 2.40 and 1. 77 eV respectively.

Catalytic activity

Methylation of phenol was carried out in vapour phase silica reactor with 3g of catalysts. Prior to reaction, the catalysts were activated at 500°C for 2 h in flowing air. The products were analysed by a GC 15 A gas chromatograph fitted with FID and a FAP – S- 10 % on 60/80 Chromosorb W (AW) column.

Results and Discussion

Physico-chemical characteristics of the catalysts

Pure dysprosia prepared by hydroxide method was colourless. Impregnation with vanadia imparted a pale yellow colour to the supported systems, the intensity of the colour deepened as the concentration of vanadia is increased. The physico-chemical characteristics of the supported systems are presented in Table 1.

Table 1—Physico-chemical characteristics of supported vanadia systems

Catalyst	Vanadia %	Average particle size (nm)	BET S. A (m^2/g)	Pore volume (cm^3/g)
D	0	23	21.9	0.83
D3	3.0	15	26.1	0.90
D7	7.9	19	23.3	0.78
D11	11.5	26	18.7	0.68
D15	14.8	31	18.0	0.65
V_2O_5	100	30	2.6	0.02

X-ray diffraction studies

X-ray diffraction enables the identification of various crystalline phases in the catalyst samples. Figure 1 depicts the XRD patterns for the supported system along with that of pure support and crystalline vanadia. For pure Dy_2O_3, prominent reflections were observed at 2θ values 28.9, 14.30, 33.4, 20.21 and 33.6° with corresponding *d* spacing values 3.08, 1.88, 2.67, 4.35 and 2.66Å. A comparison of the XRD patterns shows that no reflections due to crystalline V_2O_5 are detected in the supported catalysts even at higher percentage of vanadia, while new peaks characteristic of $DyVO_4$ appeared. Crystalline V_2O_5 showed peaks at 2θ values 20.2, 26.2, 31, 18.4 and 33.6°, with corresponding *d* spacing values 4.38, 3.40, 2.88, 5.76 and 2.61Å respectively. Peaks arising from $DyVO_4$ were detected at 2θ values 24.9, 33.35, 49.5, 18.6 and 35.45°, with *d* spacings 3.57, 2.68, 1.83, 4.76 and 2.53Å respectively. This is in accordance with the report that basic oxides favour compound formation with vanadia[8]. The relative intensity of the respective peaks indicated a progressive increase of dysprosium *ortho*-vanadate with vanadia addition. The mean crystallite size of the catalysts were calculated from the broadening of an X-ray diffraction peak, following the Scherrer method (Table 1).

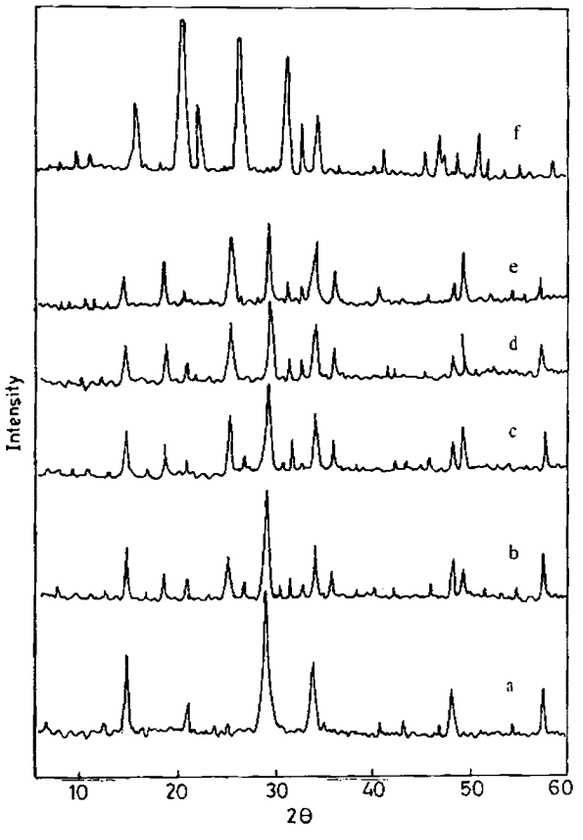

Fig. 1—XRD patterns of vanadia supported samaria. [a—Dy_2O_3 ; b—3% V_2O_5 ; c—7% V_2O_5 ; d—11% V_2O_5 ; e—15% V_2O_5; f—V_2O_5].

FTIR spectral studies

Fourier Transform IR spectrum is identified as a very useful tool for analyzing the structure of the amorphous species in the supported catalysts. Spectra of the systems calcined at 500°C are provided in Fig. 2. IR and XRD data also prove the absence of crystalline vanadia. The presence of crystalline vanadate in the supported system is confirmed by the broad band at ~ 800 cm^{-1} region, which account for the VO_4^{3-} entity that results from the dysprosium *ortho*-vanadate[14]. This supports the conclusion that dysprosia form compounds with vanadia. A very weak band is observed in the spectrum of the supported catalysts at 1065 cm^{-1}, which is associated with amorphous vanadia species on the surface. The surface species of vanadium is identified as monooxo species. A dioxo species (O=V=O) when present gives several combination bands as reported by Wachs[15]. The possibility of poly vanadyl surface species is also ruled out from the absence of V=O stretching frequencies in the 1000 – 950 cm^{-1} region[16]. Thus isolated monooxo vanadyl group on the surface of dysprosia is apparent. Region at ~ 3500 cm^{-1} exhibits broad band due to surface hydroxyl groups. As seen from the spectra, there is a shift in the region of the band to lower frequency for the supported system. According to the reports by Boehnm *et al.* the IR band at higher frequency corresponds to the most basic hydroxyl group and the

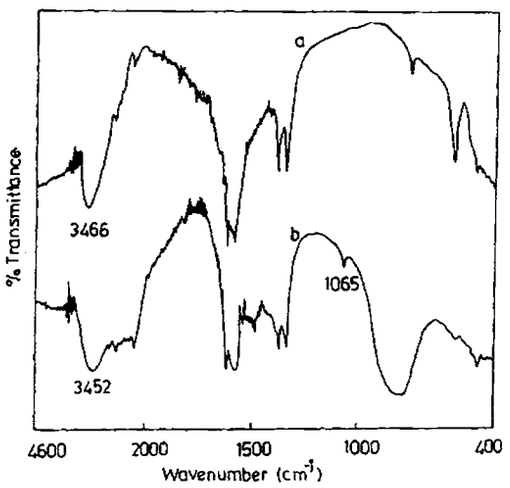

Fig. 2—FTIR spectra of a) Dy_2O_3 and b) D15

decrease in frequency of the surface hydroxyl group is associated with increasing acidity[17]. This ensures that basic OH groups on the surface are participating in bond formation with the vanadia species.

Based on the information perceived from the FTIR spectra, the structure of amorphous vanadia can be drawn. The surface metal oxide species coordinate to the oxide surface by titrating the basic surface hydroxyls of Dy_2O_3. As mentioned earlier, vanadia exists as isolated monooxo species in the supported system. It has been well established that monooxo vanadyl units exist as isolated tetrahedra on the surface of vanadia supported systems[18-20]. So the dispersed vanadia can be assigned a structure as shown in Scheme 1. The proposed structure explains the FTIR spectral band observed at 1065 cm^{-1}, which originates from the V=O stretching vibration. Due to the interaction with the surface, this band is shifted to higher wavenumber region when compared with the band position of V=O in pure vanadia.

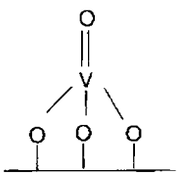

Scheme 1

Thermal studies

For pure lanthanide oxide, an initial weight loss is observed in 100-200°C region, which corresponds to loss of adsorbed water and/or water of crystallization. In the 250-350°C range, the transformation $La(OH)_3 \rightarrow LaOOH \rightarrow La_2O_3$ takes place. Further heating leads to removal of adsorbed surface carbonates, which is formed as an effect of strong interaction of basic lanthanide oxides with atmospheric CO_2 during preparation[21-23]. In the case of supported systems, two distinct weight losses are observed in the thermogram. DTG pattern also supported this conclusion. The initial weight loss in the 100-200°C region represents loss of physisorbed water or water of crystallisation. Further weight loss, which occurs in the 350-450°C range, corresponds to loss of surface hydroxyls since the percentage of rare earth oxide is high in supported samples. Besides, formation of orthovanadate is also taking place in this region as observed by Olevia and coworkers[24]. No further weight loss was observed upto 800°C and the system was found to be highly stable. DTA profile also agrees well with these observations, showing two endothermic peaks in the above regions.

Surface area and pore volume

Surface area of the samples calcined at 500°C is given in Table 1. Addition of 3% V_2O_5 induced an initial enhancement of surface area of the system, which may be due to the dispersion of vanadia over the support. Higher vanadia content reduced the surface area, probably due to the formation of crystalline dysprosium orthovanadate and the dispersion of vanadia into bulk of the catalyst system.

Pore volume values presented in Table 1 show a trend similar to surface area with percentage of vanadia. According to Dubinin's classification of pore diameter[25], a major portion of the pores was distributed in the macropore range with a few in mesoporous region. Micropores were found to be absent. A reduction of pores in the macropore region and a shift to mesoporous region is observed by depositing vanadia on Dy_2O_3 due to decrease of pore radii as a result of vanadia incorporation.

Electron donating property (Lewis basicity)

In adsorption method, the strength and distribution of basic sites are followed by the adsorption of electron acceptors (EA)[26-28]. Electron donating capacity is a measure of Lewis basicity, since during adsorption, transfer of electrons from the catalyst surface to the adsorbate occurs generating radical anions. The extent of electron transfer depends on the nature of electron donor (basic) sites and the electron affinity of the electron acceptors. The electron donor strength of a surface is defined as the conversion power of an adsorbed electron acceptor to its anion radical. If the electron affinity of the electron acceptor is high, it can accept electrons even from very weak donor sites and if the value is low, it will prefer only strong donor sites. If electron affinity of the EA is too poor, there is no formation of radical anion on the surface. Hence the strength of electron donor sites can be expressed as the limiting electron affinity value, at which free radical anion formation is not observed. Using electron acceptors with different electron affinity values, the distribution of base sites on the surface can be understood.

For the catalyst systems, PDNB adsorption was too negligible indicating the absence of very strong basic sites. Electron donor adsorption imparted characteristic colouration to the catalyst surface suggesting the formation of radical anions of TCNQ and chloranil. On pure Dy_2O_3, TCNQ adsorption

developed a bluish green colour and chloranil a pale pink colour. In the case of supported catalysts, which were pale yellow coloured, pale green and pale grey colours developed for TCNQ and chloranil respectively. Limit of electron transfer in terms of electron affinity value of the EA is not altered by vanadia impregnation. From the langmuir plots obtained, limiting amount of EA adsorbed on each of these systems was determined (Fig. 3). Since TCNQ is a stronger EA, leading to adsorption on both weak and strong donor sites, limiting amount adsorbed is higher in the case of TCNQ adsorption. Chloranil forms radical anions only on comparatively stronger basic sites, resulting in low adsorbed amount. The reduction in concentration of both strong and weak sites due to vanadia loading is evident from data in Table 2. It can be inferred that consumption of strong basic sites are predominant due to vanadia loading.

It is obvious from the adsorption data that the limiting amount of electron acceptor adsorbed is in the order 0 > 3 > 7 >11 > 15 wt % of vanadia. Since this trend is a measure of electron transfer, it is assumed that vanadia incorporation decreases the Lewis basicity of the support, which is in accordance with Le Bars and coworkers' observation[29]. Earlier work on adsorption of electron acceptors have well ascertained the role of surface hydroxyl ions and surface O^{2-} centers as electron donor sites on the oxides. At higher activation temperatures, trapped electron centers also function as electron donor sites[30,31]. But in the present case, the probability of electron defect centers was ruled out since they were created at an activation temperature > 500°C (ref. 32). So major contribution towards basic sites arises from surface hydroxyl ions. Hence the data clearly reveal that basic OH groups on the dysprosia are getting utilized for the bond formation with the vanadia species. For pure samaria the hydroxyl band was seen at 3462 cm^{-1}. The position of the characteristic band shifted to lower frequencies with progressive addition of vanadia. D15 system gave maximum deviation, in which the hydroxyl band was observed at 3448 cm^{-1} (Fig. 2).

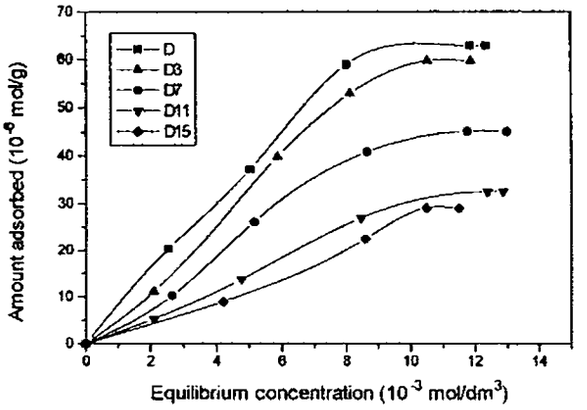

Fig. 3—Langmuir adsorption isotherms

Ammonia TPD studies

Ammonia introduction was followed by evacuation for 15 min to eliminate weakly adsorbed hydrogen bonded ammonia. Measurements were taken from 100°C onwards in order to avoid the weak interaction due to physisorption. Below 100°C, the amount of ammonia desorbed was too high indicating the capacity of the samples to physisorb a large quantity of ammonia. Auroux *et al.*[33] reported the same behaviour with rare earth oxides. Temperature programmed desorption profile for the catalyst systems are given in Fig. 4. Two major peaks are observed in the acid site distribution curves. The area of the peaks corresponds to the acid amount in that particular temperature range. Amount desorbed from lower temperature region corresponds to weaker acidic sites, while that at higher region denotes strong sites. It is difficult to speculate about the exact nature of acidic sites by simple TPD study. However, in the present case, it is tentatively assumed that the amount of ammonia desorbed at lower temperature represents

Table 2—Limiting amount of electron acceptors adsorbed on the supported systems

Catalyst	Limiting amount adsorbed (10^{-6} mol/m^2)	
	TCNQ	Chloranil
D	3.55	2.86
D3	2.69	2.09
D7	2.53	1.93
D11	2.15	1.73
D15	1.90	1.61

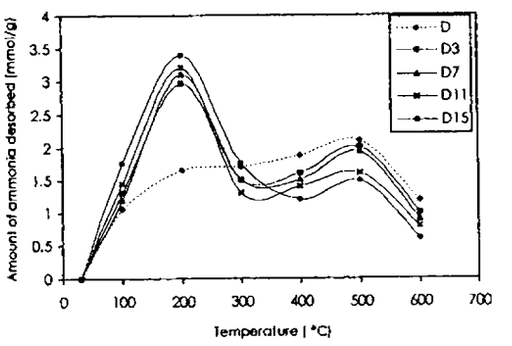

Fig. 4—Temperature programmed desorption curve of the catalysts

Bronsted acidity. This is supported by the fact that evacuation of probe molecule adsorbed surface at > 300°C removes most of the bases from Bronsted acid sites[33,34]. Coordinately bound ammonia, which has strong interaction with the surface site, can be desorbed only at higher temperatures and hence the amount of ammonia desorbed at higher temperatures is considered to be due to ammonia bound on Lewis acid sites.

Figure 4 clearly indicates that upon vanadia addition, amount of ammonia desorbed at lower temperature region is increased and that at higher temperature region is decreased considerably. As per the explanations given above, there is an enhancement in Bronsted acid sites. Reports which show that Bronsted acidity is created even when the support lacks any such sites are available[35]. Wachs also supported the generation of Bronsted acid sites at higher vanadia loadings[15]. Surface OH groups are confirmed to be one of the factors that contribute to acidity[36]. But in the case of supported systems, this is applicable at low vanadia loadings, where Bronsted acidity doesn't appear. At this point, explanation by Turek *et al.* is relevant, where Bronsted acidity was attributed to a crowding effect due to increase of surface density of molecularly dispersed species observed at higher loadings of the supported oxides[37]. Turek proposed that the simplest conceivable model of Bronsted acid site that can be proposed here consists of two surface species sharing a common proton located between two oxygens belonging to two different V – O – Support fragments. Bornsted acidity is created independent of the structures of the proton connected surface metal oxide units if they are in the privileged configuration to each other. In the case of rare earth supported vanadia, 3% by wt. of vanadia itself increases the Bronsted sites to a significant extent, after which there is no remarkable change. This means that the crowding effect might have reached by the addition of 3% vanadia itself. Further vanadia loading may be initiating the *ortho*-vanadate formation.

The decrease of Lewis acid sites with progressive vanadia addition is clear from the TPD curve. Kantcheva *et al.* attributed Lewis acidity to cations of the support in the case of supported systems[38]. In the present system, coordinately unsaturated dysprosium ions play the role of Lewis acid sites. So it can be inferred that Lewis acid sites resulting from exposed cations of dysprosia are being consumed upon vanadia addition. Evidences exist for the participation of Lewis acid sites of the support in the bond formation with vanadium species[39].

Cyclohexanol decomposition reaction

For a better appreciation of the influence of vanadia on the acidity of dysprosia, vapour phase decomposition of cyclohexanol was carried out. Selectivity in alcohol decomposition reactions has long been regarded as one of the indirect methods for investigating acid base property of metal oxides[40-43]. The amphoteric character of the alcohols permits their interaction with acidic and basic sites. Dehydrogenation takes place with the intervention of both acidic and basic sites and dehydration takes place with the participation of acidic sites. As a consequence, dehydration rate could be taken as a measure of acidity, while the ratio of dehydrogenation rate to dehydration rate as a rough index of the basicity[40]. Decomposition of cyclohexanol yield cyclohexene (dehydration product) and cyclohexanone (dehydrogenation product) as major components. Apart from these, the reaction also gave minor amount methyl cyclopentene (MCP) by the isomarisation of cyclohexene due to the interaction with strong acid sites of the catalyst. The effect of vanadia on the selectivity gives a clue regarding the nature of the sites in the supported systems. Pure Dy_2O_3 exhibited higher selectivity for dehydrogenated product, showing the presence of strong basic sites on the support. Besides, rare earth oxides possess a large amount of Lewis acid sites, which take part in dehydrogenation. Both TPD and electron donating property study have revealed the reduction of Lewis acid and base sites in the supported system, which leads to low selectivity for cyclohexanone, since both of these take part in dehydrogenation. Data in Table 3 shows that, vanadia addition brings about a dramatic enhancement in the selectivity of dehydration products. Bezouhanava *et al.* recommended the Bronsted acid sites to be responsible for catalyzing dehydration of cyclohexanol to cyclohexene[41]. It is in agreement with the results obtained from the TPD studies that vanadia incorporation induces an increase of Bronsted acid sites. It is apparent that the selectivity of dehydration products doesn't vary significantly as the composition of vanadia varies from 3 to 15 wt%. Data on TPD studies also show no significant variation for Bronsted sites after D3. The addition of vanadia beyond 3%, may not be increasing the Bronsted acidity significantly or the Bronsted acid sites may not be sufficiently strong for catalyzing cyclohexene formation.

Catalytic activity

Reaction of methanol with phenol is a reaction, catalysed by both acid and basic sites. Both O- and C-alkylated products are derived from the reaction, which include anisole, methyl anisole, *o*-cresol, different isomers of xylenol, trimethyl phenols etc., which constitute industrially important intermediates in the manufacture of plastics, pesticides, pharmaceuticals etc.[44,45]. Most important ones among this category are *o*-cresol and 2,6-xylenol, the former is used in the manufacture of epoxy cresol novalak resins, where as 2,6-xylenol is a monomer of a good heat resisting poly-(2,6-dimethyl) phenylene oxide resin[46].

Catalytic activity of the supported vanadia system is presented in Table 4. Anisole, *o*-cresol, 2,6-xylenol and trimethyl phenol (TMP) costitute the main products. Traces of methyl anisole were also detected. Major fraction of the products includes ring-alkylated phenols, which indicate catalysis of C-alkylation by Dy_2O_3/V_2O_5. The activity shows a variation directly proportional to the vanadia content in the supported system. From Table 4 it is seen that the increase of vanadia concentration induced the formation of higher alkylated phenol with a corresponding decrease of *o*-cresol.

Influence of acid base properties on product selectivity

In general, basicity was found to have an adverse effect on the catalytic activity towards phenol alkylation. It was found from adsorption of electron acceptors that basicity follows the order D3> D7 > D11 >D15. The opposite trend is followed for the conversion of phenol. Higher concentration of ring-alkylated products indicates that weak acidic/strong basic sites are present in the supported system. Earlier workers have reported that weak acid/strong basic sites favour C-alkylation[47-50].

According to earlier studies, the acid base property of the catalyst has a pronounced effect on the *ortho* selectivity in the methylation of phenol. For the present system, *ortho* selectivity (*o*-cresol, 2,6-xylenol and methyl anisole) decreased with vanadia addition. It can be understood in terms of decrease of basicity as confirmed by studies on the adsorption of electron acceptors. This is in agreement with Tanabe[51] that basic catalysts alkylate selectively at *ortho* position. Accordingly, the *o*-selectivity should be proportional to basic strength. Nevertheless, contradictory reports exist in literature that acidic catalysts predominantly alkylate *ortho* position[8].

Klemm *et al.* proposed the following mechanism (shown in Scheme 2) for phenol alkylation[10]. Phenol interacts with Lewis acid base centers giving phenolate ion (on Lewis acid site) and H^+ (on basic site). This proton induces formation of carbonium ion from methanol, which interact with the adsorbed phenolate ion at *ortho* positions

The decrease in the *ortho* product selectivity can be understood in these lines also. It was confirmed through acid base property studies that both Lewis

Table 3—Cyclohexanol decomposition data over Dy/V system

[Reaction conditions : Catalyst = 2.5 g; Reaction temp. = 623 K; Feed rate = 6 ml / h, TOS = 1 h]

Catalyst	Conversion (%)	Product distribution (%)			Selectivity (%)	
		MCP	Cyclohexene	Cyclohexanone	C=C	C=O
D	42.3	—	12.89	29.85	30.12	69.88
D3	31.4	7.37	79.92	12.71	87.29	12.71
D7	33.0	9.77	77.69	12.54	87.46	12.54
D11	34.3	9.91	77.75	12.52	87.48	12.52
D15	44.0	12.21	75.94	11.86	87.14	11.86

Table 4—Conversion and selectivity of products in the methylation of phenol on Dy/V system

[Reaction conditions : Reaction temperature : 350°C; Phenol : methanol ratio : 1: 7; Flow rate : 4 ml/h; TOS : 1.5 h.]

Catalyst	Conversion (%)	Selectivity (%)				
		Anisole	Me anisole	*o*-cresol	2,6-xylenol	TMP
D3	29.5	4.1	-	72.1	21.2	2.6
D7	47.1	2.1	-	55.3	35.1	7.5
D11	68.1	2.6	-	42.6	36.5	8.3
D15	73.5	5.1	13.3	25.5	44.9	11.1

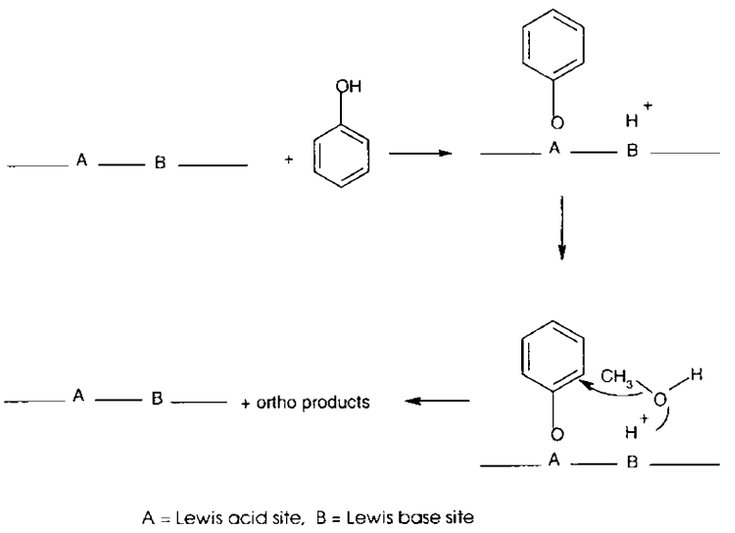

Scheme 2—Adsorption of phenol on Lewis site

acidity and Lewis basicity are decreasing with increase of vanadia loading, which leads to decrease of *ortho* products. Besides, at higher vanadia loaded catalysts, Bronsted acid sites generated interact with benzene ring yielding higher methylated phenols as suggested by Tanabe *et al.*[11]. According to them Bronsted sites interact with the electron cloud of benzene ring. So ring will be parallel to the surface giving access to positions other than *ortho* for attack by alkylating group.

Reaction pathway

Reaction pathways for methylation include direct ring alkylation and intramolecular rearrangement of O-methylated products to yield C-alkylated products[12]. Alkylation over acidic catalysts was supposed to proceed through anisole formation, which rearranges intramolecularly to give *o*-cresol. Stronger acidic sites favour *meta* and *para* cresols. Xylenol formation occurs via consecutive methylation of cresol. On the other hand, basic and bifunctional catalysts adopt direct ring alkylation route. *Ortho* product selectivity is found to be high on basic systems by direct ring alkylation. It has been well established that conversion of phenol is directly proportional to basicity if the reaction proceeds through the rearrangement of an anisole intermediate. In contrast basicity has an adverse effect on the activity if direct C-alkylation is taking place. Hence direct ring alkylation is expected to take place on the supported system without the formation of anisole intermediate. From the data in Table 4, it is clear that *ortho* cresol selectivity decreases with vanadia addition. 2,6-Xylenol selectivity first increases followed by a decrease as the vanadia content is increased, whereas TMP selectivity goes on increasing. Hence it can be inferred that *ortho* cresol formed undergoes consecutive methylation to give higher alkylated phenols.

Acknowledgement

The authors wish to acknowledge CSIR, New Delhi for the award of SRF to NKR.

References

1 Le Bars J, Auroux A, Forisier M & Vedrine J, *J Catal*, 162 (1996) 250.
2 Eon J G, Olier R & Volta J, *J Catal*, 145 (1994) 318.
3 Jonathan C Otamari & Arne Anderson, *Catal Today*, 3 (1988) 211.
4 Dines T J, Rochester C H & Wars A M, *J Chem Soc Faraday Trans*, 87 (1991) 1473.
5 Sohn J R, Cho S G, Pae V I & Hayashi S, *J Catal*, 159 (1996) 170.
6 Lopez-Nieto J M, Kremenik G & Fiero J G, *Apll. Catal* 61 (1990) 235.
7 Chaar M, Patel D, Kung M & Kung H H, *J Catal*, 109 (1988) 463
8 Corma A, Lopez Nieto J M, Paredes N, Perez M, Shen Y, Cao H & Suib S L, *Stud Surf Sci Catal*, 72 (1992) 213.
9 Rao V V, DurgaKumari V & Narayanan S, *Appl Catal*, 49 (1989) 165.
10 Klemm L H, Klopfenstein C E & Shabtai J, *J Org Chem*, 35 (1970) 1069.

11 Tanabe K, Nishizaki K, in F.C. Tompkins (Ed), *Proc. 6 th Int. Congress on Catalysis* (The Chemical Society, London) 1977.
12 Santhaccasia E, Galosa D & Carra S, *Appl Catal*, 64 (1990) 83.
13 Narayana K V, Venugopal A, Rama Rao K S, Venkat Rao V, Khaja Masthan S & Kanta Rao P, *Appl Catal A*, 150 (1977) 269.
14 Gadsden J A, *IR spectra of minerals and related compounds*, (1975) p.26.
15 Wachs I E, *Catal Today*, 27 (1996) 437.
16 Frederickson Jr L D & Hausen D M, *Anal Chem*, 35 (1963) 818.
17 Boehnm H P & Knozinger H, edited by J R Anderson & M Moudart, *Catalysis* (Springer, Berlin) Vol. 4, 1983, Chapter 2.
18 Eckert H & Wachs I W, *J Phys Chem*, 93 (1989) 6796.
19 Xingtao Gao, Fierro J LG & Wachs I E, *Langmuir*, 15 (1999) 3169.
20 Blasco T & Lopez Nieto J M, *Appl Catal A:Gen*, 157 (1997) 117.
21 Rosynek M P & Magnusun D T, *J Catal*, 46 (1977) 402.
22 Ambrozhi M N & Dvornikova L M, *Zh Neorg Khim*, 11 (1966) 86.
23 Rosynek M P & Magnusun D T, *J Catal*, 48 (1977) 417.
24 Oliveira H P, Anaissi F J & Toma H E, *Material Research Bulletin*, 33 (1998) 1783.
25 Dubinin M M, *Chem Rev*, 60 (1960) 235.
26 Esumi K & Meguro K, *J colloid interface Sci*, 66 (1) (1978) 192.
27 Sugunan S & Rani G D, *J Mat Sci Lett*, 10 (1991) 887.
28 Porter R P & Hall W K, *J Catal*, 5(1966) 366.
29 Le Bars J, Vedrine J C, Auroux A, Trautman S & Baerns M, *Appl Catal A: Gen*, 119 (1994) 341.
30 Esumi K & Meguro K, *J Adhesion Sci Technol*, 4 (1990) 393.
31 Meguro K & Esumi K, *J colloid interface Sci*, 59 (1) (1977) 93.
32 Flockhart B D & Leith I R, Pink R C, *Trans Faraday Soc*, 65 (1969) 542.
33 Auroux A & Gervasini A, *J Phys Chem*, 94 (1990) 6371.
34 Hatayama F, Ohno T, Maruoka T, Ono T & Miyata H, *J Chem Soc Faraday Trans*, 87 (16) (1991) 2629.
35 Sohn J R, Cho S G, Pae Y I & Hayashi S, *J Catal*, 159 (1996) 170.
36 Bernholc J, Horseley J A, Murrell L L, Sherman L G & Soled S J, *J phys Chem*, 91 (1987) 1526.
37 Turek A M, Wachs I E & De Canio E, *J phys Chem*, 96 (1992) 5000.
38 Kantcheva M M, Hadijiivanov K I & Klissurski D G, *J Catal*, 134 (1992) 299.
39 Das N, Eckert H, Hu H, Wachs I E, Walcer J & Feber F, *J phys Chem*, 97 (1993) 8240.
40 Mamoru Ai, *Bull chem Soc Japan*, 50 (10) (1997) 2579.
41 Bezouhanava C P & Al – Zihari M A, *Catal Lett*, 11 (1991) 245.
42 Rosynek M P, Koprowski R J & Dellisante G N, *J Catal*, 122 (1990) 80.
43 Narasimhan C S & Swamy C S, *Appl Catal*, 2 (1982) 315.
44 Fiege H, *Ullmann's Encyclopedia of Industrial Chemistry*, edited by B Elvers, S Hawkins & G Schultz, 5th Edn (VCH Verlag) 1991, Vol A19, p. 313.
45 Narayanan S, *Res Ind*, 34 (1989) 296.
46 Dowbenko R, edited by J I Kroschwit & Mary Houl-Grant Kirk Othmer *Encyclopedia of chemical Technology*, 4th Edn, Vol 2, 1992, p. 106.
47 Rao V V, Chari K V R, DurgaKumari V & Narayanan S, *Appl Catal*, 6 (1990) 89.
48 Benzouhanava C & Al-Zihari M A, *Appl Catal*, 8 (1992) 45.
49 Marczewski M, Bodibo J P, Perof G & Guisnel M, *J Mol Catal*, 50 (1989) 211.
50 Tliemat-Manzalji R T, Bianchi D B & Pajonk G M, *Appl Catal* 101(1993) 339
51 Tanabe K, *Catalysis by acids and bases (Stud surf sci catal*, Vol.20), edited by B Imelik, C Naccahe, G Coudurier,Y B Taarit & J C Vedrine (Elsevier, Amsterdam),1985, p-1.